# $Ni(OH)_2$ nanodots decorated Co-Co LDH/C hollow nanocage for high performance supercapacitor

Yuan Yang[a], Xiuqin Wang[b], Feifei Huang[a], Jialu Zhao[c], Xiuhua Wang[a]*

[a]College of Chemistry and Materials Science, Anhui Normal University, The Key Laboratory of Functional Molecular Solids, Ministry of Education, Anhui Laboratory of Molecular-Based Materials, Key Laboratory of Electrochemical Clean Energy of Anhui Higher Education Institutes, Wuhu 241002, China

[b]Shandong Provincial Cancer Hospital and Institute, Jinan 250117, China

[c]Central South University of Forestry and Technology, Changsha 410004, China

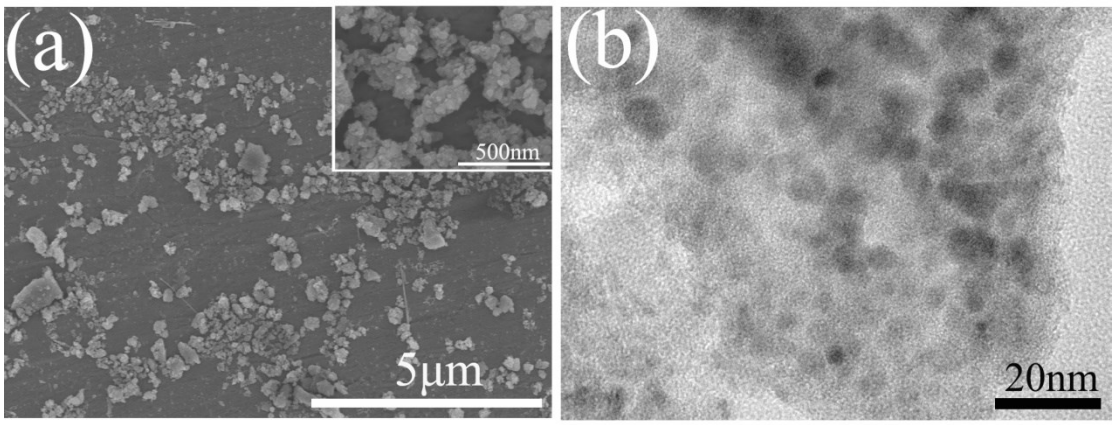


Fig. S1. (a) SEM and (b) TEM images of $Ni(OH)_2$.

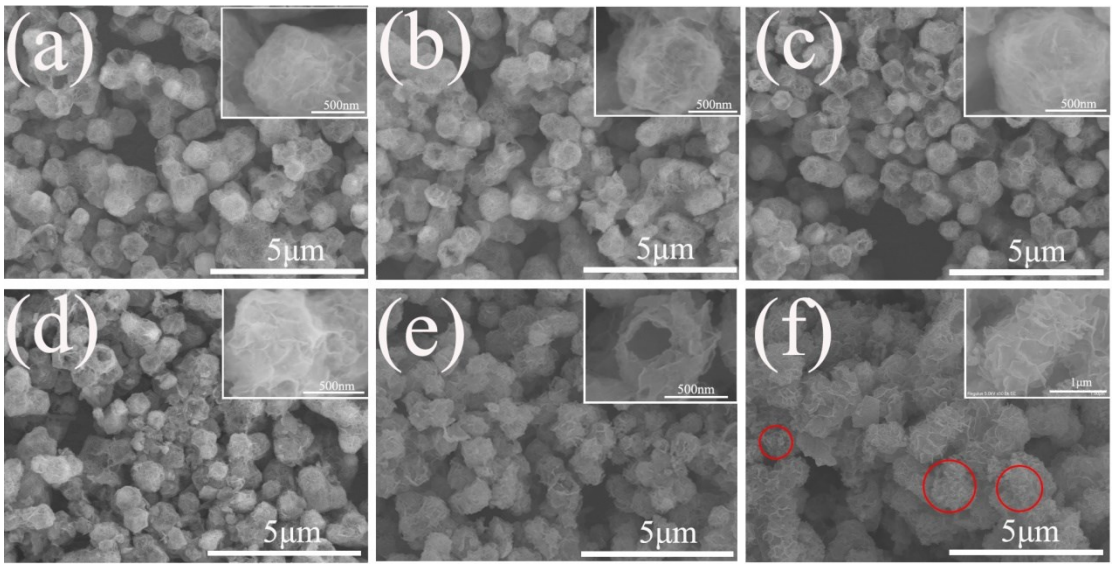


Fig. S2. SEM images of (a) Co-Co LDH/C/$Ni(OH)_2$-10, (b) Co-Co LDH/C/$Ni(OH)_2$-20, (c) Co-Co LDH/C/$Ni(OH)_2$-30, (d) Co-Co LDH/C/$Ni(OH)_2$-40, (e) Co-Co LDH/C/$Ni(OH)_2$-50 and (f) Co-Co LDH/C/$Ni(OH)_2$-60.

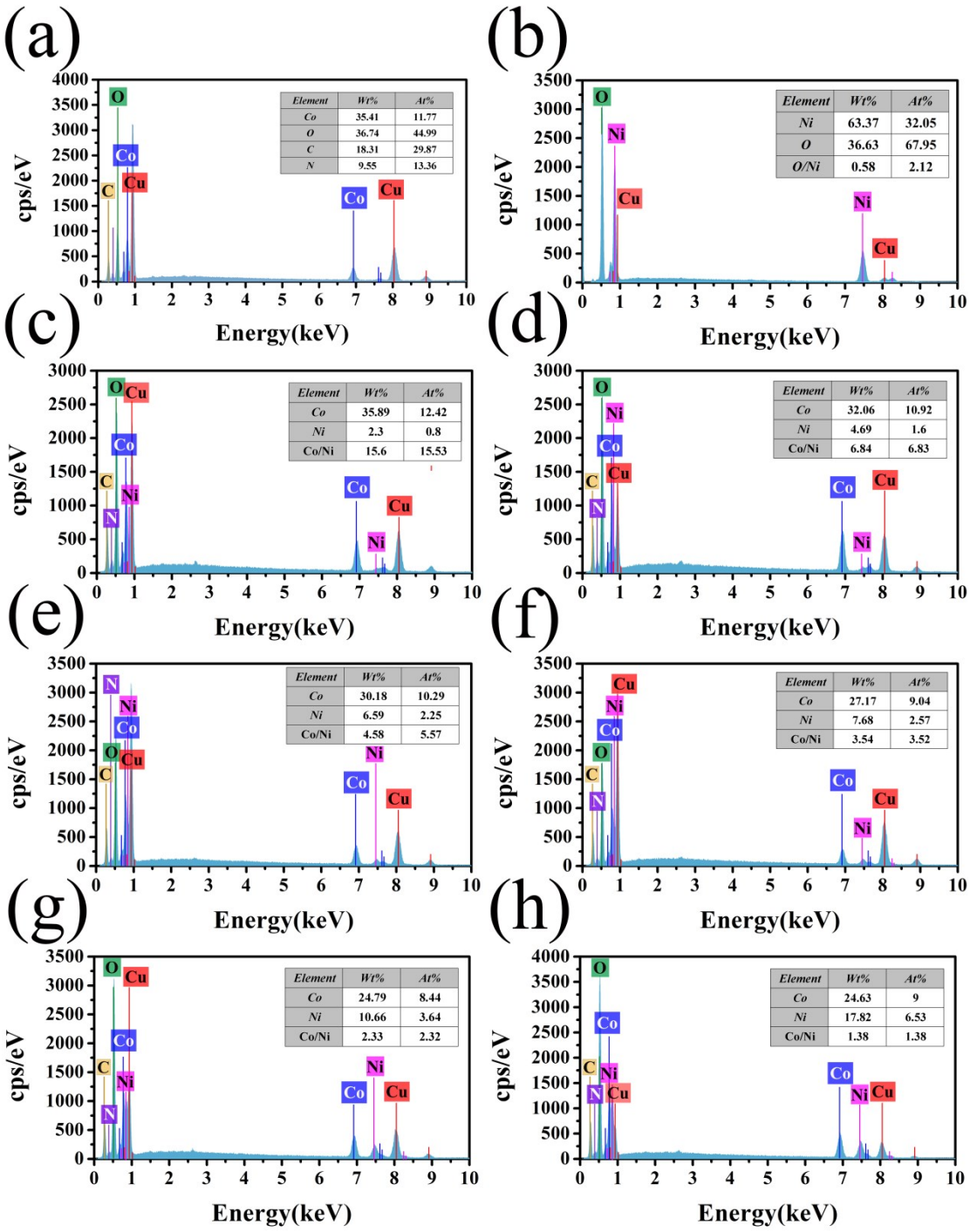


Fig. S3. EDS spectra of (a) Co-Co LDH/C, (b) $Ni(OH)_2$, (c) Co-Co LDH/C/$Ni(OH)_2$-10, (d) Co-Co LDH/C/$Ni(OH)_2$-20, (e) Co-Co LDH/C/$Ni(OH)_2$-30, (f) Co-Co LDH/C/$Ni(OH)_2$-40, (g) Co-Co LDH/C/$Ni(OH)_2$-50 and (h) Co-Co LDH/C/$Ni(OH)_2$-60.

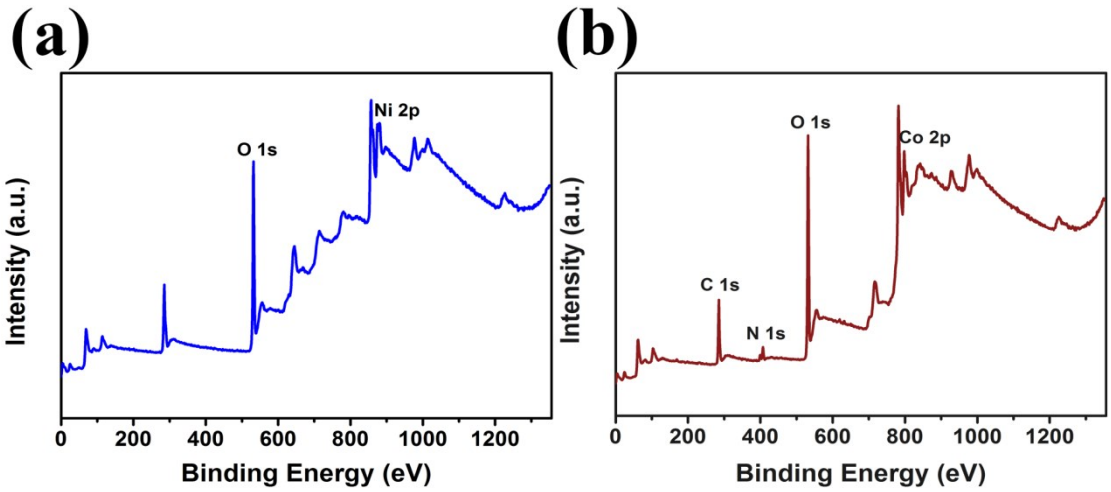


Fig. S4. XPS survey spectra of (a) $Ni(OH)_2$ and (b) Co-Co LDH/C.

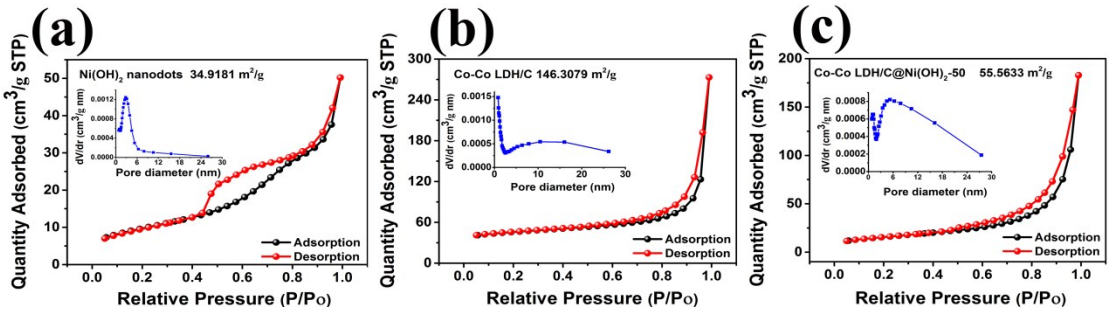


Fig. S5. $N_2$ adsorption-desorption isotherms and corresponding pore size distribution plots (inset) of (a) $Ni(OH)_2$ nanodots, (b) Co-Co LDH/C and Co-Co LDH/C@$Ni(OH)_2$-50.

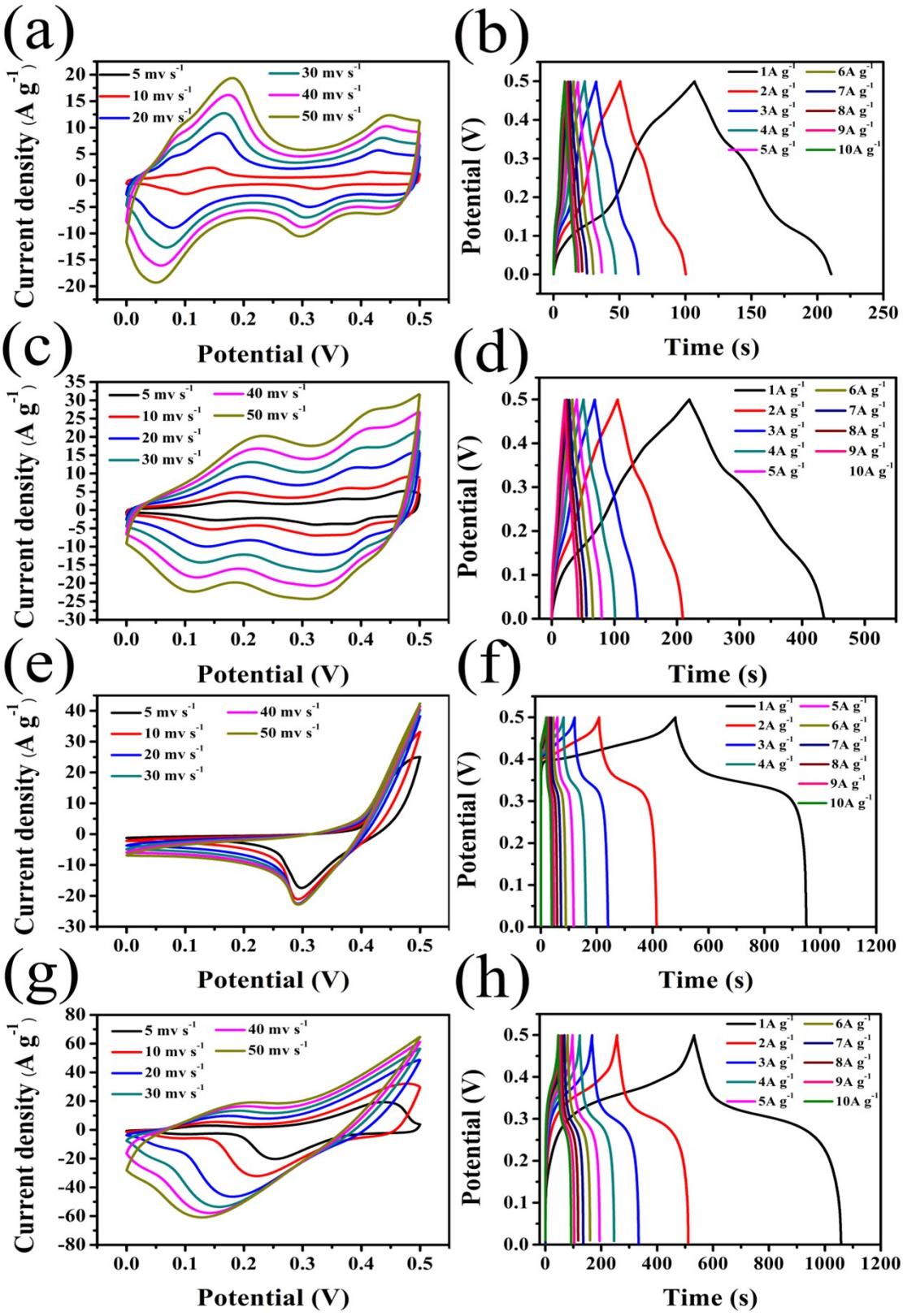


Fig. S6. CV curves at different scanning speeds for (a) Co-Co LDH, (c) Co-Co LDH/C, (e) $Ni(OH)_2$ and (g) Co-Co LDH/$Ni(OH)_2$-50; GCD profiles at various current densities for (b) Co-Co LDH, (d) Co-Co LDH/C, (f) $Ni(OH)_2$ and (h) Co-Co LDH/$Ni(OH)_2$-50.

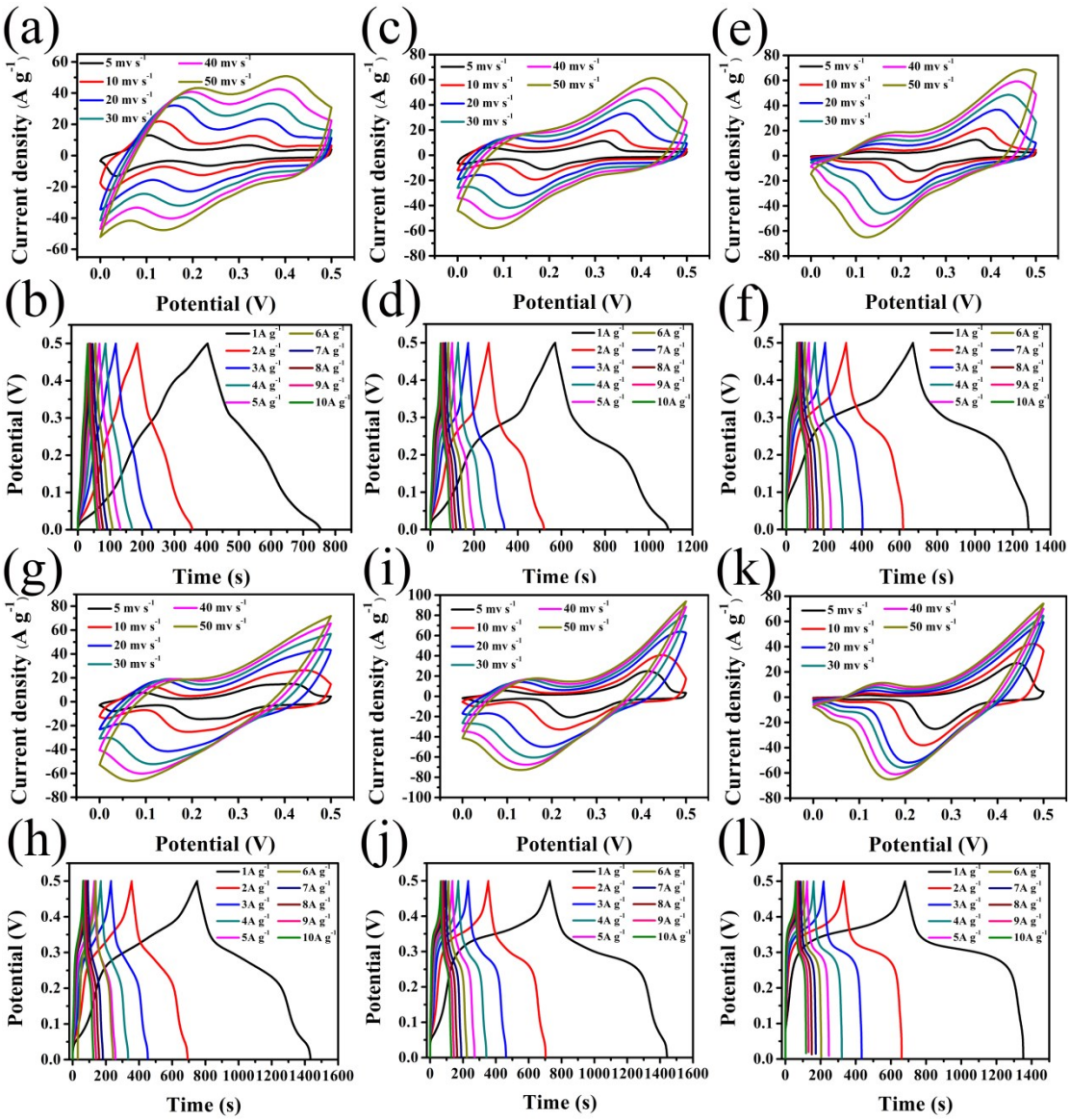


Fig. S7. CV curves at different scanning speeds for (a) Co-Co LDH/$Ni(OH)_2$-10, (c) Co-Co LDH/$Ni(OH)_2$-20, (e) Co-Co LDH/$Ni(OH)_2$-30, (g) Co-Co LDH/$Ni(OH)_2$-40, (i) Co-Co LDH/$Ni(OH)_2$-50 and (k) Co-Co LDH/$Ni(OH)_2$-60; GCD profiles at various current densities for (b) Co-Co LDH/$Ni(OH)_2$-10, (d) Co-Co LDH/$Ni(OH)_2$-20, (f) Co-Co LDH/$Ni(OH)_2$-30, (h) Co-Co LDH/$Ni(OH)_2$-40, (j) Co-Co LDH/$Ni(OH)_2$-50 and (l) Co-Co LDH/$Ni(OH)_2$-60.

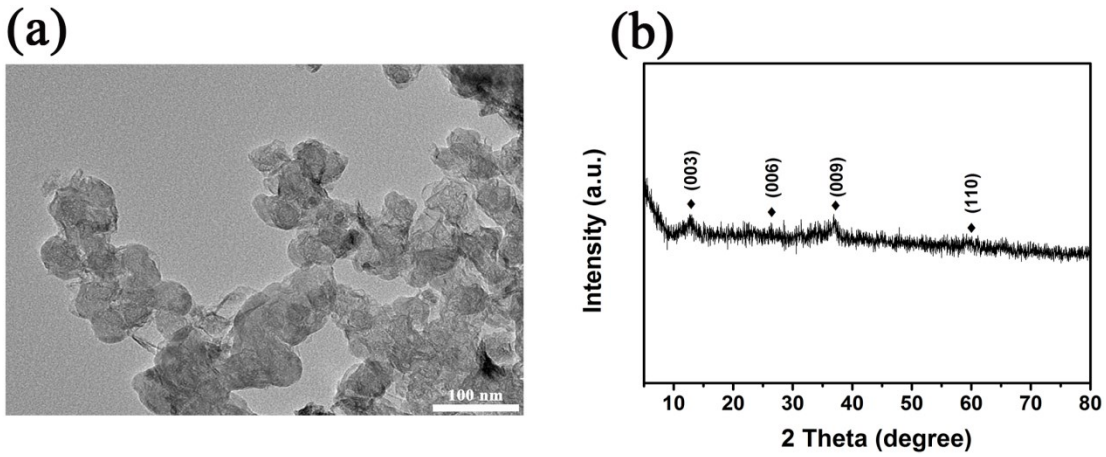


Fig. S8 (a) the TEM image of Co-Co LDH/$Ni(OH)_2$-50 electrode after 3000 cycling; (b) the XRD pattern of Co-Co LDH/$Ni(OH)_2$-50 electrode after 3000 cycling.

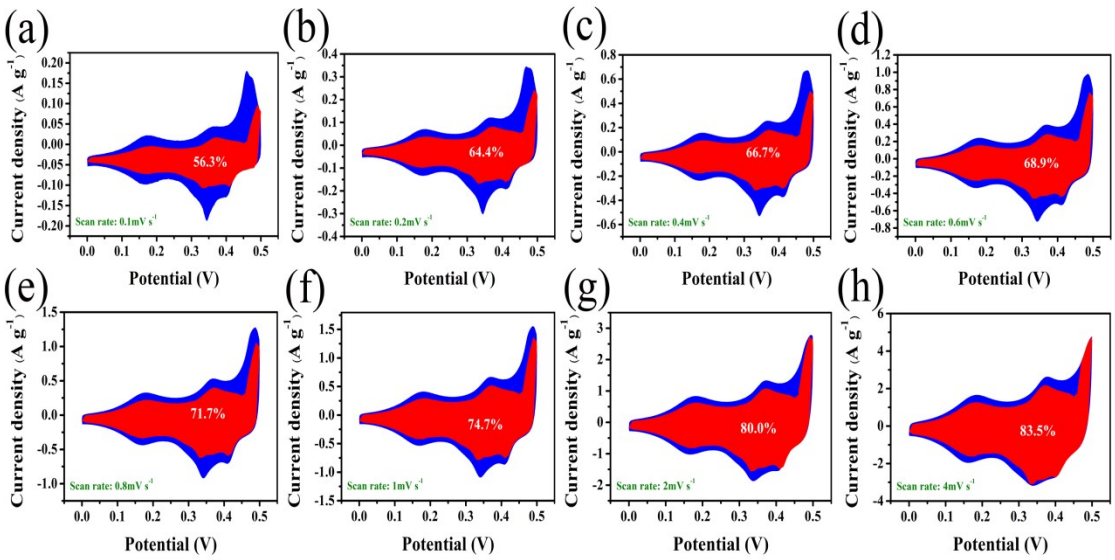


Fig. S9. The capacitive contribution to charge storage of Co-Co LDH at different scan rates of (a) 0.1, (b) 0.2, (c) 0.4, (d) 0.6, (e) 0.8, (f) 1, (g) 2 and (h) 4 mV $s^{-1}$.

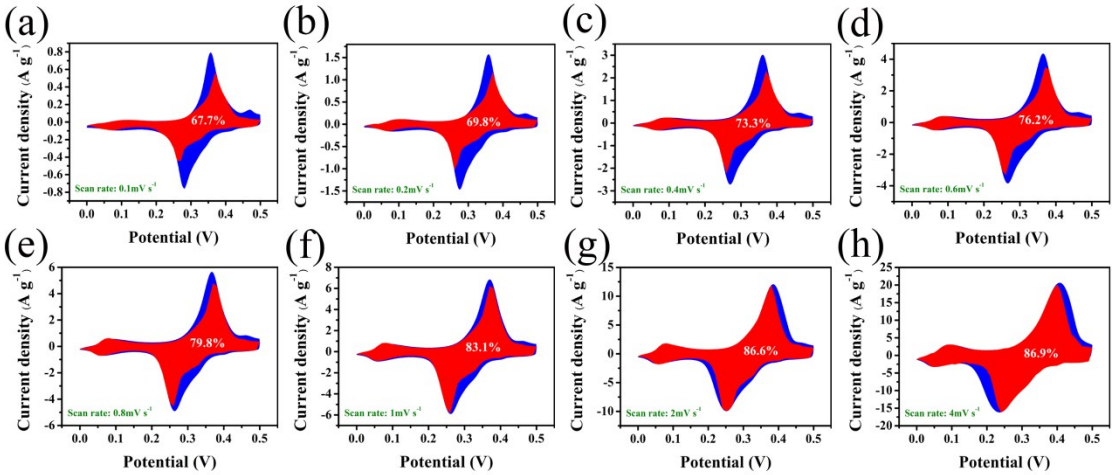


Fig. S10. The capacitive contribution to charge storage of Co-Co LDH/C/Ni(OH)$_2$-50 at different scan rates of (a) 0.1, (b) 0.2, (c) 0.4, (d) 0.6, (e) 0.8, (f) 1, (g) 2 and (h) 4 mV s$^{-1}$.

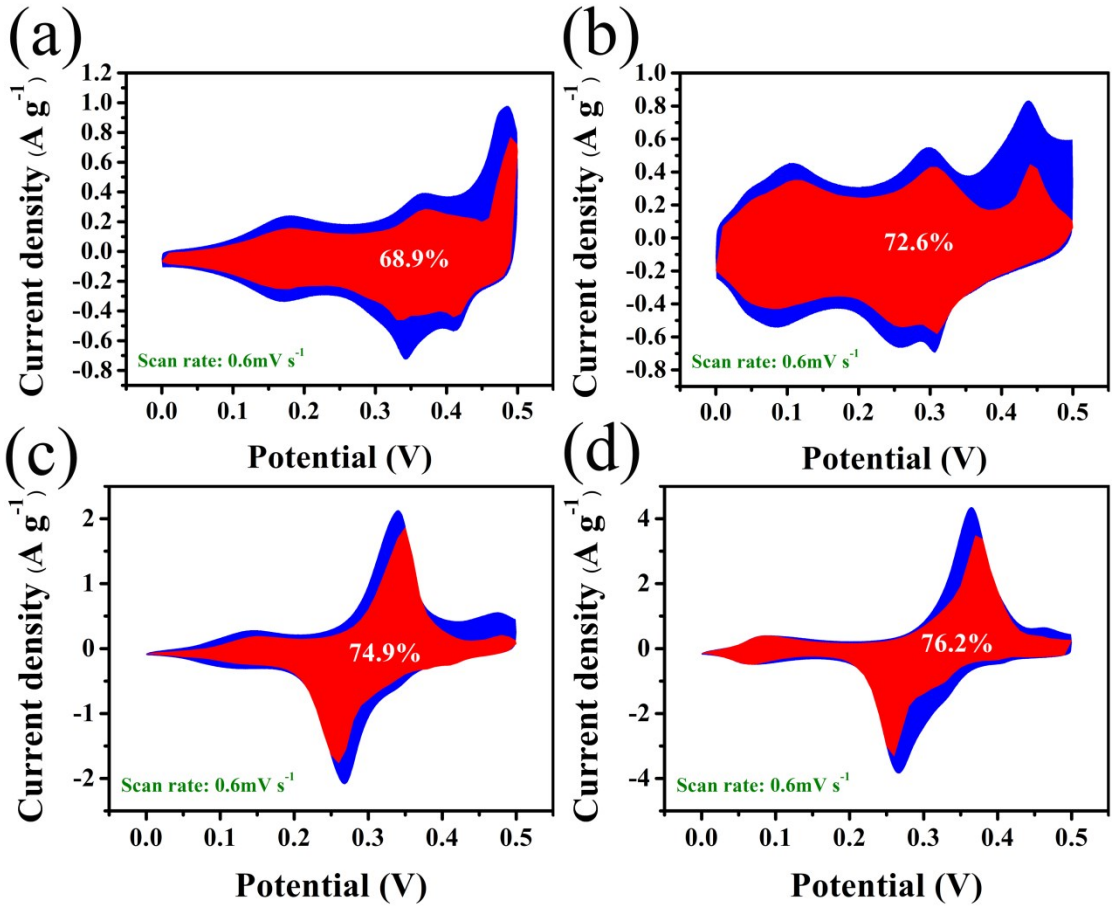


Fig. S11. Capacitive contribution of charge storage of Co-Co LDH/$Ni(OH)_2$ composites with different $Ni(OH)_2$ contents (0, 10, 30 and 50 wt.%) at a scan speed of 0.6mV $s^{-1}$.

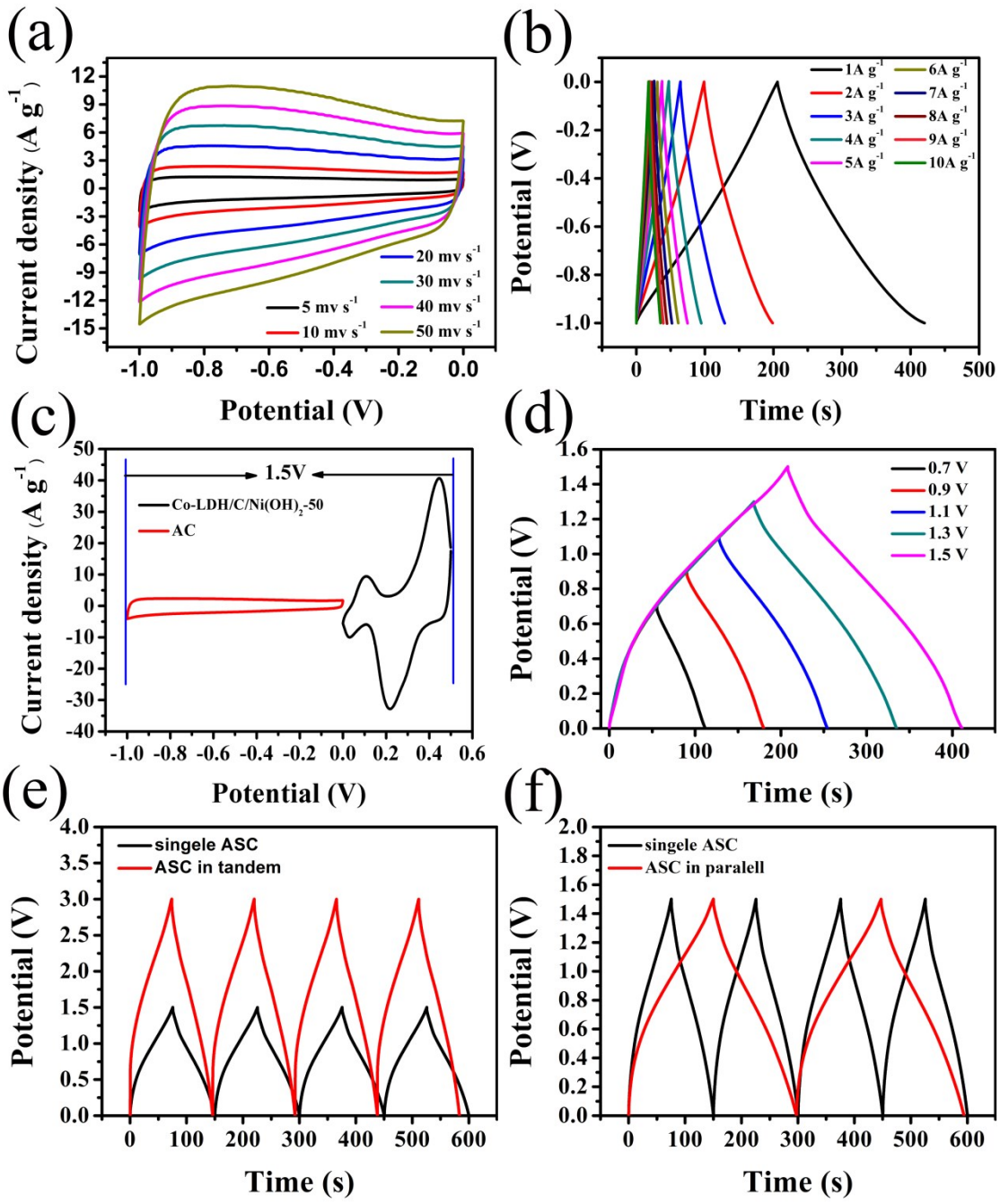


Fig. S12. (a) CV curves at various scan rates, (b) GCD profiles at various current densities for AC. (c) Cyclic voltammograms of AC and Co-Co LDH/C/$Ni(OH)_2$-50 in three electrode configurations against SCE electrode showing corresponding operational voltage window. (d) GCD curve of Co-Co LDH/C/$Ni(OH)_2$-50//AC Hybrid supercapacitor under different potential windows. Two pieces of Co-Co LDH/C/$Ni(OH)_2$-50//AC (e) tandem and (f) parallel GCD curves compared to a single Co-Co LDH/C/$Ni(OH)_2$-50//AC.

Table S1. Comparison of our work with previously reported work

| Electrode material | Specific capacitance | Capacitance Retention | Cycling stability | References |
|---|---|---|---|---|
| **$Ni(OH)_2$@Co/C** | 952 F $g^{-1}$ at 0.5A $g^{-1}$ | 80% (from 0.5-10 A $g^{-1}$) | — | [1] |
| **CNT@$Ni(OH)_2$** | 1251 F $g^{-1}$ at 1A $g^{-1}$ | 78.4% (from 1-100 A $g^{-1}$) | 75% after 2000 cycles | [2] |
| **$Ni_xCo_{1-x}(OH)_2$** | 1000 F $g^{-1}$ at 5 mV $s^{-1}$ | 69.9% (from 5-500 mV $s^{-1}$) | 100% after 1000 cycles | [3] |
| **$ZnCo_2O_4$@$Ni(OH)_2$** | 1021 F $g^{-1}$ at 1 mA $cm^{-2}$ | 55.3% (from 1-10 mA $cm^{-2}$) | 50.1% after 5000 cycles | [4] |
| **Ni(OH)2/CoO/rGO** | 1317 F $g^{-1}$ at 2 A $g^{-1}$ | 66% (from 2-10 A $g^{-1}$) | 84.8% after 2000 cycles | [5] |
| **$Ni(OH)_2$/a-GCA** | 1342.5 F $g^{-1}$ at 1 A $g^{-1}$ | 78.4% (from 1-10 A $g^{-1}$) | 79% after 5000 cycles | [6] |
| **Co-Co LDH/C/$Ni(OH)_2$-50** | 1426 F $g^{-1}$ at 1 A $g^{-1}$ | 90.2% (from 1-10 A $g^{-1}$) | 81.1% after 3000 cycles | Our work |

References:


[1] X. Li, Y. Qiao, C. Wang, T. Shen, X. Zhang, H. Wang, Y. Li and W. Gao, *J. Alloy. Compd.*, 2019, **770**, 803-812.

[2] Y. Yang, Y. Zhou, Y. An, Q. Zhang, X. Wang, X. Yang and Z. Hu, *J. Phys. Chem. Solids*, 2018, **119**, 126-137.

[3] J.-C. Chen, C.-T. Hsu and C.-C. Hu, *J. Power Sources*, 2014, **253**, 205-213.

[4] X. Han, Y. Yang, J.-J. Zhou, Q. Ma, K. Tao and L. Han, *Chem.-Eur. J.*, 2018, **24**, 18106-18114.

[5] L. Jiang, R. Zou, W. Li, J. Sun, X. Hu, Y. Xue, G. He and J. Hu, *J. Mater. Chem. A*, 2013, **1**, 478-481.

[6] Y. Zhang, W. Fan, H. Lu and T. Liu, *Electrochim. Acta*, 2018, **283**, 1763-1772.